

Copper–dioxygen chemistry and modeling the Fe–Cu center in cytochrome *c* oxidase

Kenneth D. Karlin,* Stephen Fox, Alaganandan Nanthakumar, Narasimha N. Murthy, Ning Wei, Honorio V. Obias and Constantinus F. Martens

Department of Chemistry, Charles and 34th Streets, The Johns Hopkins University, Baltimore, Maryland 21218, U. S. A.

Abstract

The copper(I) complex [(TMPA)Cu(RCN)]⁺ (**1**) binds O₂ forming [(TMPA)Cu]₂(O₂)²⁺ (**2**), with *trans*-μ-1, 2 peroxo-coordination. Ligands with quinolyl groups substituting for the pyridyl donors in TMPA cause dramatic changes in the course of reaction, in one case stabilizing a Cu/O₂ 1:1 adduct [(BQPA)Cu(O₂)]⁺ (**6**). The kinetics/thermodynamics are compared. Reaction of **1** with (F₈-TPP)Fe(II)pip₂ (**8**) and O₂ yields the μ-oxo species [(F₈-TPP)Fe^{III}-O-Cu^{II}(TMPA)]⁺ (**9**); this reversibly protonates giving μ-hydroxo bridged [(F₈-TPP)Fe-(OH)-Cu(TMPA)]²⁺ (**12**). The novel NMR properties of **9** are described. These complexes are discussed in terms of their model O₂-chemistry in hemocyanins or cytochrome *c* oxidase.

INTRODUCTION

Copper ion is an essential trace element found in living systems, with its primary importance being its role in mediating or catalyzing chemical reactions at the active sites of proteins or enzymes. Copper proteins perform a diverse array of functions, all involving oxidation-reduction (i.e. 'redox') activity, since the types of ligands typically found in protein matrices facilitate, in particular, redox shuttling between reduced copper(I), and copper(II) oxidation states. These ligands include side-chain imidazole groups of histidine, the phenol oxygen atom in tyrosine, or the sulfur in cysteine. Protein active-site copper ions carry out electron transfer reactions, for example as electron carriers in photosynthetic organisms. Many other copper proteins effect redox reactions which involve atom transfer, such as those involving the processing of molecular oxygen (Table 1) or nitrogen oxides (1-3).

TABLE 1. Main classes of copper proteins involved in O₂-processing.

PROTEIN	SOURCE	BIOLOGICAL FUNCTION
<u>Oxygen Carrier</u>		
Hemocyanin (Hc)	Molluscs and Arthropods	O ₂ -transport
<u>Copper Monooxygenases</u>		
Tyrosinase (Tyr)	Fungal, Mammal	Tyrosine oxygenation
Dopamine β-hydroxylase (DβH)	Adrenal, Brain	Dopamine → Norepinephrine
Peptidylglycine α-Amidating Monooxygenase (PAM)	Pituitary, Heart	Oxidative N-dealkylation
Phenylalanine Hydroxylase (PAH)	<i>Chromobacterium violaceum</i>	Phenylalanine → Tyrosine
Methane Monooxygenase (MMO)	Methanogenic bacteria	Methane → Methanol
Ammonia Monooxygenase	bacteria	NH ₃ → NH ₂ OH
<u>Copper Dioxygenases</u>		
Quercetinase	Fungal	Quercetin oxidative cleavage
<u>Copper Oxidases</u>		
Ascorbate Oxidase (AO)	Plants	Oxidation of L-Ascorbate
Laccase	Tree, Fungal	Phenol and diamine oxidation
Ceruloplasmin	Human, animal serum	weak oxidase activity
Amine oxidase	most animals	elastin, collagen formation
Galactose oxidase	Molds	Galactose oxidation
Cytochrome <i>c</i> Oxidase (CcO)	Mitochondria	Terminal oxidase (Proton pump)
<u>Other</u>		
Superoxide Dismutase (SOD)	Red blood cells, animals	O ₂ ⁻ detoxification

Hemocyanins are blood O_2 -transporting proteins (Fig. 1), while monooxygenases effect reactions involving oxygen-atom insertion into C-H bonds. Oxidases carry out oxidation or dehydrogenation of organic substrates, accompanied by O_2 -reduction to either hydrogen peroxide or water. Cytochrome *c* oxidase is a the mitochondrial terminal oxidase involved in O_2 -reduction to water concomitant with energy transduction via proton pumping. An important copper/zinc superoxide dismutase (*SOD*) is well characterized, and recent evidence suggests that a point mutation in the *SOD* gene may cause a degenerative disease of motor neurons, the inherited form of amyotrophic lateral sclerosis (*ALS*) (4).

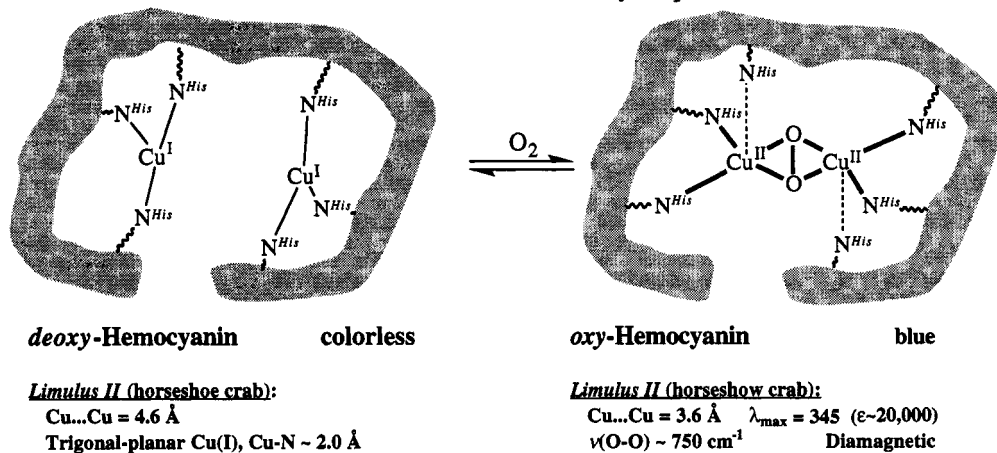
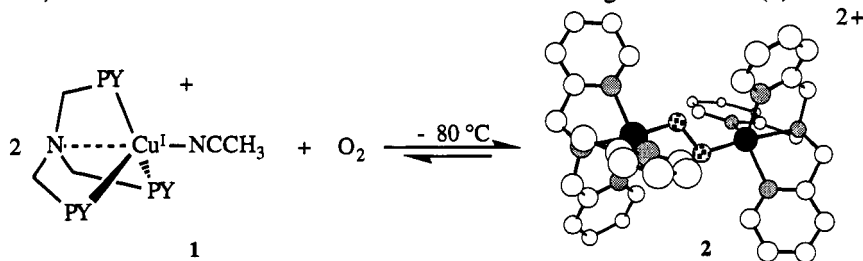


Fig. 1. Reversible binding of O_2 by hemocyanins, with key physical properties.

We, and others have endeavored to understand the structure and function of copper proteins involved in copper(I)/ O_2 interactions, by studying inorganic models, i.e., synthetically derived copper(I) complexes and their O_2 -reactivity (2,3,5). Such biomimetic approaches can lead to fundamental insights into the metal-based chemistry, leading to an improved understanding of biological O_2 -activation mechanisms, and the dependence of reactivity patterns upon the specific nature of Cu_n-O_2 structure. One might also envision the development of reagents or catalysts for use in practical oxidation processes. Here, we will highlight recent findings concerning the reversible binding of dioxygen to certain copper(I) complexes. We also wish to describe chemistry related to the dinuclear iron-copper center in cytochrome *c* oxidase (*CcO*), where an oxo-bridged dinuclear porphyrin-iron-copper complex can be generated either by dioxygen interaction with reduced iron-porphyrin and copper complexes, or via acid-base reactions.

O_2 -CHEMISTRY OF $Cu(I)$ COMPLEXES CONTAINING TRIPODAL LIGANDS

In order to model the neutral, aromatic, nitrogenous imidazolyl character observed in the histidyl-copper coordination found in hemocyanin and many other copper proteins, some of our studies have utilized synthetically accessible tripodal, tetradentate chelating pyridyl ligands, such as TMPA (TMPA = tris[(2-pyridyl)methyl]amine). The first X-ray structurally characterized Cu_2O_2 species, the *trans*- μ -1,2-peroxo [((TMPA)Cu) $_2(O_2)]^{2+}$ (**2**), was formed from the reaction of [(TMPA)Cu(RCN)] $^+$ (**1**) (PY = 2-pyridyl) with O_2 at -80°C in EtCN or CH_2Cl_2 (Cu: O_2 = 2:1, manometry). The Cu(II) ions in **2** are pentacoordinate, the Cu-Cu distance is 4.359 Å and the O-O bond length is 1.432 Å (6).

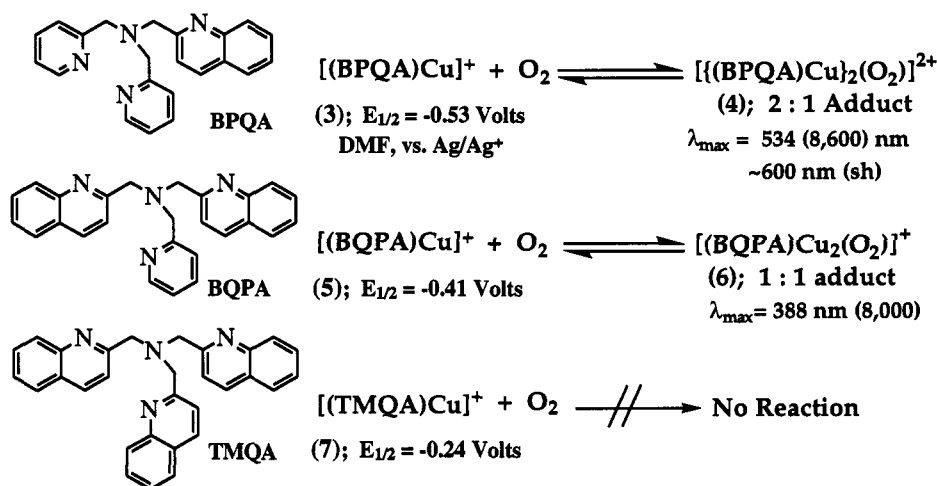


[((TMPA)Cu) $_2(O_2)]^{2+}$ (**2**) is intensely purple as a solid or in solution where it displays multiple strong absorptions at $\lambda_{\text{max}} = 440 \text{ nm}$ ($\epsilon = 2000 \text{ M}^{-1}\text{cm}^{-1}$), 525 nm (11500), and 590 nm (sh, 7600), all assigned to O_2^{2-} to Cu(II) charge-transfer transitions. In addition, there is a d-d band at 1035 nm (180). Although

O₂ binds strongly to complex **1** at low temperature, it can be removed reversibly by vacuum cycling experiments, i.e., application of vacuum while the solution is subjected to brief heating. Resonance Raman studies of **2** show a O-O stretch (832 cm⁻¹) and a Cu-O stretch (561 cm⁻¹) (6b). Complex **2** also exhibits silent EPR and nearly normal ¹H NMR spectra. Magnetic susceptibility measurements performed on **2** indicate that $-2J > 600$ cm⁻¹, based on $\mathbf{H} = 2JS_1S_2$. These results show that a single bridging O₂²⁻ ligand can mediate strong magnetic coupling between two Cu(II) ions. Although **2** is a functional model for hemocyanin, it lacks the precise spectroscopic and structural signatures of the active site of oxy-hemocyanin (vide supra), wherein $\eta^2:\eta^2$ O₂²⁻ to dicopper(II) binding has been determined (7). Kitajima and coworkers (3) have achieved the synthesis of a model compound with the exact structure observed in oxy-hemocyanin, using sterically hindered tris(pyrazolyl)borate tridentate ligands.

Quinolyl Analogues of TMPA and their Cu(I)/O₂ Chemistry

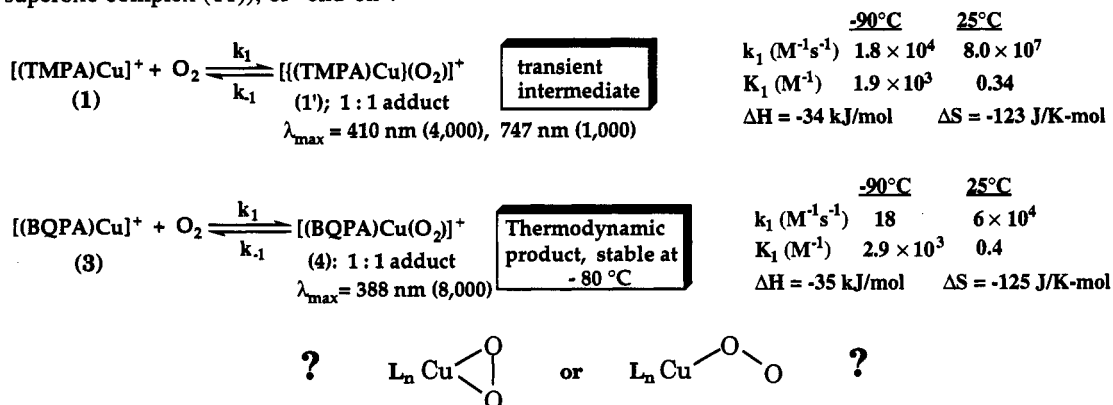
The chemistry of substituting quinolyl for pyridyl groups on the TMPA framework has proven particularly insightful in probing the effects of ligand donor steric and/or electronic effects in the resulting LCu(I)/O₂ chemistry, where L = BPQA, BQPA or TMQA. As increased numbers of quinolyl groups are placed into the complexes, there is a dramatic effect upon the apparent stoichiometry of reaction with dioxygen. [(BPQA)Cu]⁺ (**3**) reacts similarly to the parent TMPA complex **1**, forming a low temperature stable Cu/O₂ = 2:1 adduct [(BPQA)Cu]₂(O₂)²⁺ (**4**). Quite by contrast, manometric measurements reveal that [(BQPA)Cu]⁺ (**5**) forms a 1:1 adduct [(BQPA)Cu(O₂)]⁺ (**6**), formally a superoxo-copper(II) species; its UV-vis spectrum is distinctly different ($\lambda_{\text{max}} = 388$ nm) than observed for the 2:1 adducts **2** or **4**. For [(TMQA)Cu]⁺ (**7**), with three quinolyl donors, there is no reaction with O₂ whatsoever. These observations may be seen to qualitatively correlate with the observed redox potentials for these species {E_{1/2} = -0.61 V vs. Ag/Ag⁺ in dimethylformamide (DMF) for [(TMPA)Cu(RCN)]⁺ (**1**)}, which indicate that increased quinolyl substitution thermodynamically favors the reduced copper(I) oxidation state in these complexes. However, steric effects are also likely to be important in determining the course of reaction (i.e. stoichiometry, structure, extent of reaction), and these factors are discussed elsewhere (8).



Kinetics/Thermodynamics Investigations of Pyridyl & Quinolyl-Cu(I) Complexes with Dioxygen

These observations have been confirmed in detailed kinetic/thermodynamic studies, carried out in collaboration with Prof. A. D. Zuberbühler and co-workers in Basel, Switzerland. In fact, the first kinetics-thermodynamics data for formation of a primary 1:1 adduct were determined by low-temperature stopped-flow experiments carried out on [(TMPA)Cu(RCN)]⁺ (**1**) (8a). There, a transient intermediate [(TMPA)Cu(O₂)]⁺ (**1'**) was spectroscopically observable. The kinetics parameters determined (see below) reveal that it forms very rapidly even at -90 °C, while temperature dependent activation parameters allow for an extrapolation to room temperature, showing an O₂ on-rate of $\sim 10^8$ M⁻¹s⁻¹ (8a). This compares with or exceeds the O₂-binding rate for heme proteins or model iron-porphyrin complexes (9), a variety of cobalt(II) chelate complexes, and it is comparable to the oxygenation rate of deoxy-hemocyanin (8a,10). The binding of O₂ to [(BPQA)Cu]⁺ (**3**) is slower, yet the thermodynamic parameters indicate essentially identical binding strengths for both [LCu(O₂)]⁺ adducts. The very unfavorable reaction entropies (see below) reveal why such copper-dioxygen adducts are not stable at room temperature (5,8a). The spectra of **1'** and [(BQPA)Cu(O₂)]⁺ (**6**) are rather different, indicating the strong influence of the ligand environment. Further studies are needed to better understand the nature of such Cu/O₂ 1:1 adducts

and to determine whether the superoxo-binding in these complexes is "side-on" (as seen in a cobalt-superoxo complex (11)), or "end-on".



MODELS FOR THE Fe-Cu DINUCLEAR ACTIVE SITE IN CYTOCHROME *c* OXIDASE

Cytochrome *c* oxidase (CcO) is a terminal respiratory protein which catalyzes the four-electron four-proton reduction of O_2 to water (Fig. 2). The process is coupled to proton translocation across the cell membrane. The electrochemical potential gradient generated by this proton pumping process is ultimately used in the synthesis of ATP (12). Electrons are transferred to subunit II and a so-called Cu_A center, most recently thought to consist of a dinuclear mixed-valent Cu center. A low-spin heme a_3 is also involved in electron transfer, but the critical O_2 -reduction site is the dinuclear metal site which consists of a high-spin heme a_3 and closely neighboring Cu_B . The latter possesses minimally three $\text{N}_{\text{histidyl}}$ donor ligands.

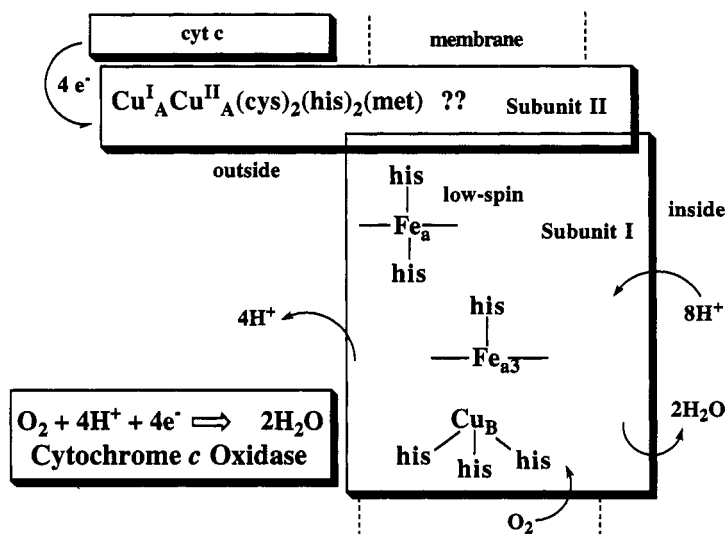


Fig. 2. A representation of the CcO enzyme with its multiple metal centers.

Considerable biochemical and inorganic modeling research efforts have focused on aspects of the 'as-isolated' resting oxidized state of the dinuclear center, which possesses a strongly spin-coupled ($-J > 50 \text{ cm}^{-1}$) $\text{Fe}^{\text{III}}\text{-X-Cu}^{\text{II}}$ center. The nature and the identity of the bridging ligand which mediates the antiferromagnetic coupling between the metal centers is not yet clear. However, μ -chloro, μ -sulfido, μ -imidazolato and μ -oxo groups have been proposed as possible bridging ligands (12,13).

With our experience with copper(I)/ O_2 chemistry, we have also been very interested in functional modeling (2,5) of CcO, i.e. O_2 -reaction chemistry involving reduced metals, with copper(I) and porphyrin-iron(II) species. For the enzyme, kinetic and spectroscopic evidence point to Cu_B as the initial binding site for O_2 , thus implicating the importance of Cu(I)-O_2 reactivity in the O_2 reduction process of CcO (12). The O_2 -ligand transfers to the heme a_3 forming an adduct analogous to that seen in hemoglobin.

Following this, the bound O₂ is rapidly converted to a peroxo-iron(III) state, which after protonation and a third electron transfer step induces cleavage of the O-O bond to generate a ferryl Fe^{IV}-oxo species. The resting oxidized state is regenerated after the fourth electron transfer and protonation.

Synthesis and Characterization of Oxo/Hydroxo Bridged Iron-Copper Dinuclear Complexes

In our initial attempts to delve into this type of chemistry, we chose to use TMPA-Cu complexes, since the O₂-reactivity of [(TMPA)Cu^I(CH₃CN)]⁺ (1) is most well understood. When an equimolar mixture of (F₈-TPP)Fe^{II}pip₂ (pip = piperidine) (8) (Fig. 3) and [(TMPA)Cu^I(CH₃CN)]⁺ (1) were allowed to react at -80° C in CH₂Cl₂ in the presence of O₂ and warmed to 0° C, a purple-red solid could be isolated by precipitation with heptane (yield > 80%). A microcrystalline solid formulated as [(F₈-TPP)Fe^{III}-(O²⁻)-Cu^{II}(TMPA)]⁺ (9) was isolated by dissolution of the crude product in acetonitrile and reprecipitation by slow addition of diethylether in an overall isolated yield of 50 %. The same complex, identified on the basis of its UV-Vis and NMR spectroscopic properties, could also be generated in an acid-base reaction, via mixing of equimolar amounts of [(TMPA)Cu^{II}(CH₃CN)]²⁺ (10), (F₈-TPP)Fe^{III}-OH (11), and Et₃N in CH₃CN (Fig. 3). An X-ray structure was obtained of a crystal generated by this latter method (13).

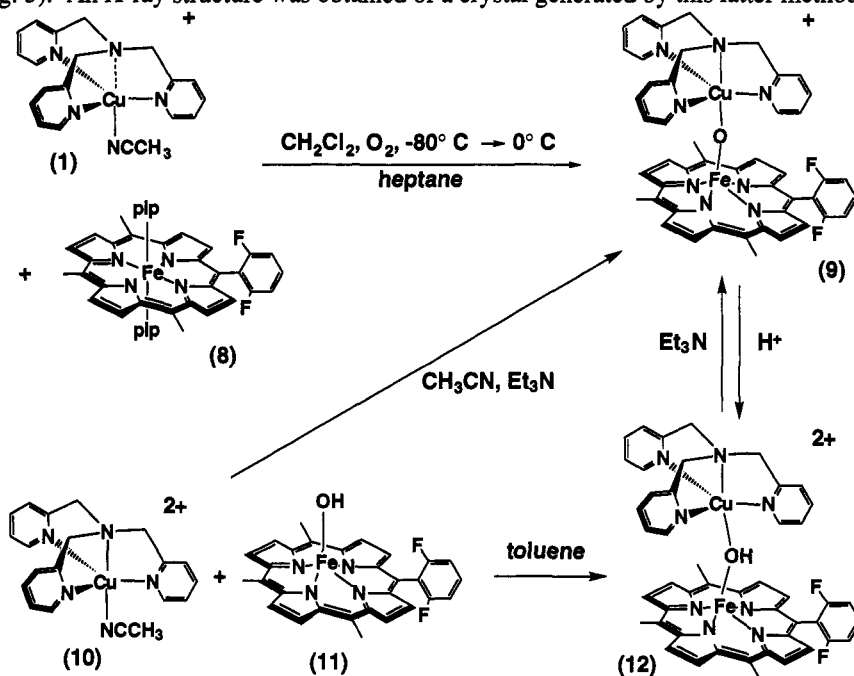
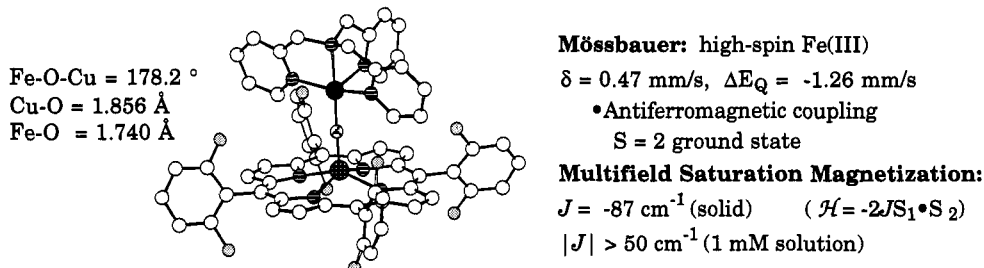


Fig. 3. Synthesis and interconversion of μ-oxo and μ-hydroxo porphyrin-iron-copper complexes.

The structure of [(F₈-TPP)Fe^{III}-(O²⁻)-Cu^{II}(TMPA)]⁺ (9) reveals a linear Fe(III)-oxo-Cu(II) coordination, with very short Fe-O and Cu-O bond lengths. The bond distances associated with the coordination of iron are similar to those reported for μ-oxo bridged iron-porphyrin dimers. The Cu coordination environment is distorted square-pyramidal; the three pyridine rings appear to sit in between the four difluorophenyl groups of the porphyrin, thereby leaving one 'slot' free (13)



Physical measurements of [(F₈-TPP)Fe^{III}-(O²⁻)-Cu^{II}(TMPA)]⁺ (9) indicate it consists of a high-spin iron(III) porphyrin strongly antiferromagnetically coupled to an S = 1/2 Cu(II) ion center, yielding a S = 2 spin system (13). Solution (~ 1 mM) magnetization data could not provide an exact value for the magnetic

coupling constant J , due to the inherent "noise" found in these measurements. These findings call into question previous evaluations for the lower limit of $|J| > -200 \text{ cm}^{-1}$ for the dinuclear Fe-X-Cu site in the "resting" CcO enzyme; a lower limit of $|J|$ greater than 50 cm^{-1} is a better estimate.

The pyrrole proton NMR signal in **9** is observed at 65 ppm (Fig. 4), shifted upfield from ~ 80 ppm relative to axially symmetric five-coordinate high-spin iron(III) tetraphenylporphyrin (TPP) complexes (14). An upfield shift is expected for an antiferromagnetically coupled system since high-spin iron(II) ($S = 2$) TPP complexes exhibit pyrrole signals in the 30-61 ppm region. The Soret band in $[(F_8\text{-TPP})\text{Fe}^{\text{III}}(\text{O}^{2-})\text{-Cu}^{\text{II}}(\text{TMPA})]^+$ (**9**) is at 434 nm, shifted from 400-415 nm, seen for typical high-spin iron(III) TPP complexes (13). Bridged μ -oxo iron-porphyrin dimers do not show a similar red-shift, indicating that the copper-TMPA moiety dramatically alters the electronic properties of the iron-oxo moiety. The IR spectrum of **9** exhibits a new band at 856 cm^{-1} , in the general region where the Fe-O-Fe antisymmetric stretch has been reported for most oxo-bridged iron complexes. Use of $^{18}\text{O}_2$ gas in the synthesis decreased the intensity of this band with corresponding changes in the $780\text{-}790 \text{ cm}^{-1}$ region. Overlapping TMPA absorptions in the region thus allow only a tentative assignment of a Fe-O-Cu antisymmetric stretch. The antisymmetric vibration of $[(F_8\text{-TPP})\text{Fe-O-Fe}(F_8\text{-TPP})]$ occurs at 867 cm^{-1} .

Protonation of $[(F_8\text{-TPP})\text{Fe}^{\text{III}}(\text{O}^{2-})\text{-Cu}^{\text{II}}(\text{TMPA})]^+$ (**9**) by addition of one equivalent of triflic acid in dichloromethane produces a new species formulated as $[(F_8\text{-TPP})\text{Fe}(\text{OH})\text{-Cu}(\text{TMPA})]^{2+}$ (**12**) (Fig. 3). The same dication could be isolated by reacting an equimolar mixture of $[(\text{TMPA})\text{Cu}^{\text{II}}(\text{CH}_3\text{CN})][\text{ClO}_4]_2$ (**10**) and $[(F_8\text{-TPP})\text{Fe-OH}]$ (**11**) in toluene or dichloromethane. This species shows a pyrrole proton NMR signal at 69 ppm in CD_2Cl_2 (compared to 65 ppm for **9**) and a solution magnetic moment of 5.5 ± 0.1 B.M. (Evans method) (13b). These data point to a weakening of coupling between the Fe and Cu centers as a result of protonation. As expected, deprotonation of **12** by addition of an equivalent of Et_3N regenerates complex **9** (Fig. 3). Preliminary X-ray Absorption (XAS) measurements on samples of **12** suggest a bent μ -hydroxo coordination with longer $\text{Cu}^{\text{II}}\text{-OH-}$ and $\text{Fe}^{\text{III}}\text{-OH-}$ bonding distances (13b).

$^1\text{H-NMR}$ Spectroscopic Properties of **9**

Other than the pyrrole 65 ppm $^1\text{H-NMR}$ resonance of $[(F_8\text{-TPP})\text{Fe}^{\text{III}}(\text{O}^{2-})\text{-Cu}^{\text{II}}(\text{TMPA})]^+$ (**9**), (*vide supra*) the $F_8\text{-TPP}$ meta (m ; 9.6 & 9.2 ppm, 8H) and para (p ; 7.8 ppm, 4H) phenyl hydrogens appear in their usual place (13a). There are four additional signals, Fig. 4, three of which are shifted upfield from

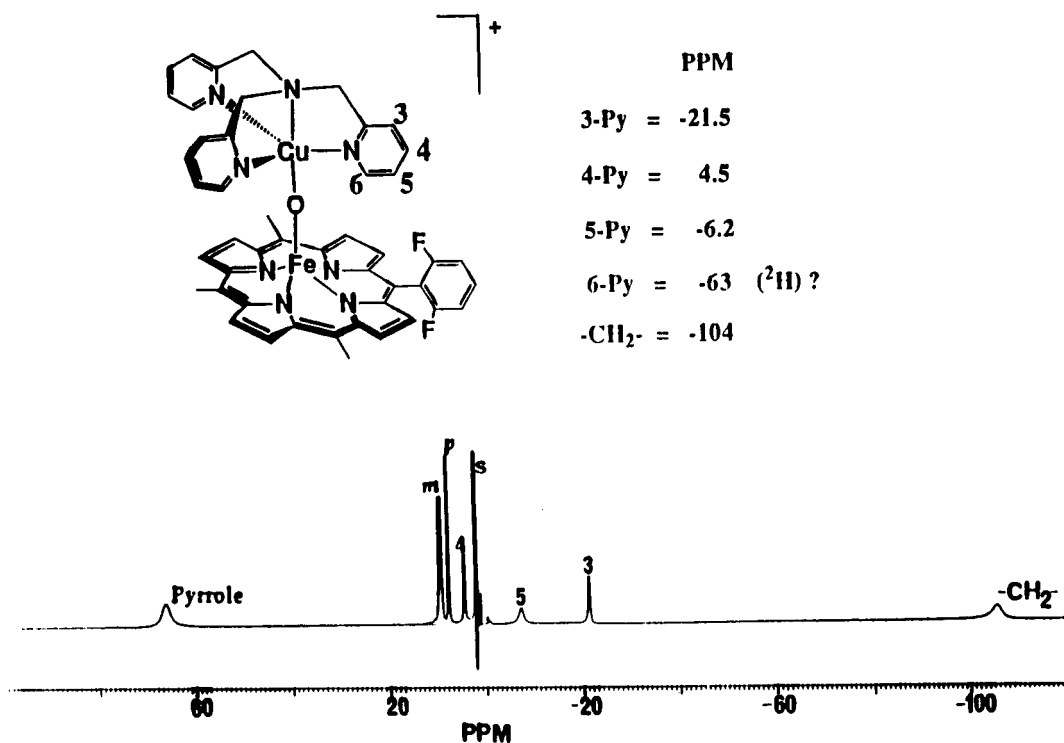


Fig. 4. $^1\text{H-NMR}$ spectrum and assignments for **9**, showing paramagnetically shifted ligand resonances.

the diamagnetic region. We recently assigned these, by carrying out syntheses of 3-, 4- or 5-methylated TMPA ligands and corresponding oxo-bridged analogues of **9**. This work has been complemented using analogues possessing deuterium-for-hydrogen substitution on the TMPA 6-pyridyl and the methylene positions. From ^1H and/or ^2H -NMR studies, the resonances are assigned as shown in Fig. 4.

Thus, the resonances on the Cu(II)-TMPA ligand shift upfield and in the opposite direction to those (i.e., the pyrrole hydrogens) on the more highly paramagnetic iron-porphyrin. These findings are novel, but have been observed in protein systems where two metals with different spins (e.g. $\text{Fe}^{\text{III}}\text{-X-Fe}^{\text{II}}$ in ferredoxins, or $\text{Cu}^{\text{II}}\text{-X-Co}^{\text{II}}$ substituted into Cu-Zn superoxide dismutase) are *antiferromagnetically* coupled (14). The observed shifts on the Cu-ligand suggest that the spin delocalization occurs predominantly via a σ -contact (through-bond) shift mechanism. Further investigations are in progress.

Possible Mechanism of Formation of **9**.

The formation of $[(\text{F}_8\text{-TPP})\text{Fe}^{\text{III}}(\text{O}^{2-})\text{-Cu}^{\text{II}}(\text{TMPA})]^+$ (**9**) by reaction of reduced porphyrin-iron(II) and copper(I) complexes, i.e., $(\text{F}_8\text{-TPP})\text{Fe}^{\text{II}}\text{pip}_2$ (**8**) and $[(\text{TMPA})\text{Cu}^{\text{I}}(\text{CH}_3\text{CN})]^+$ (**1**) (Fig. 3), at the least represents a crude functional model for cytochrome *c* oxidase, since O_2 is reduced to the oxidation state level of water in the product. Considerable efforts are underway to obtain insights into this reaction; here we offer some preliminary observations and speculations.

We have already established that $[(\text{TMPA})\text{Cu}^{\text{I}}(\text{CH}_3\text{CN})]^+$ (**1**) is very reactive to O_2 even at -80°C , forming $[(\text{TMPA})\text{Cu}]_2(\text{O}_2)]^{2+}$ (**2**) (*vide supra*), while $(\text{F}_8\text{-TPP})\text{Fe}^{\text{II}}\text{pip}_2$ (**8**) reacts only very sluggishly with dioxygen. Thus, it appears that the O_2 -chemistry in the mixed metal system is dominated by the copper(I)/ O_2 chemistry. We also observe that reacting **2** (in the absence of excess O_2) with $(\text{TPP})\text{Fe}^{\text{III}}\text{-Cl}$ gives the oxo-bridged analogue $[(\text{TPP})\text{Fe}^{\text{III}}(\text{O}^{2-})\text{-Cu}^{\text{II}}(\text{TMPA})]^+$, suggesting that reduction of Fe^{III} occurred. We confirmed this possibility; 1 stoichiometrically reduces $(\text{F}_8\text{-TPP})\text{Fe}^{\text{III}}\text{-Cl}$ to give a reactive porphyrin-iron(II) species, isolable as a toluene adduct $(\text{F}_8\text{-TPP})\text{Fe}^{\text{II}}\cdot\text{C}_7\text{H}_8$. Two equivalents of this readily reacts with $[(\text{TMPA})\text{Cu}]_2(\text{O}_2)]^{2+}$ (**2**) to give $[(\text{F}_8\text{-TPP})\text{Fe}^{\text{III}}(\text{O}^{2-})\text{-Cu}^{\text{II}}(\text{TMPA})]^+$ (**9**) in good yield, even at -80°C . Thus, we suggest that the mechanism of formation of **9** could proceed by a pathway described in Fig. 5. Either (i) $[(\text{TMPA})\text{Cu}]_2(\text{O}_2)]^{2+}$ (**2**) is directly attacked by a porphyrin-Fe(II) species present, or (ii) **2** undergoes prior O-O bond homolysis upon warming from -80°C to give to give a reactive $\text{Cu}^{\text{II}}\text{-O}\cdot$ species which combines with porphyrin-Fe(II). Regardless, the heterodinuclear oxo-bridged complex **9** forms and no μ -oxo iron dinuclear species (i.e., porphyrin-Fe-O-Fe-porphyrin) is observed. Further studies are clearly needed to better describe the reaction mechanism.

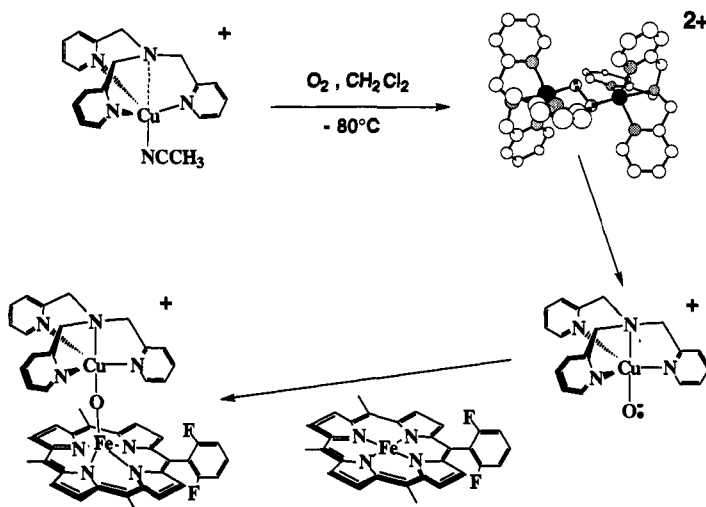
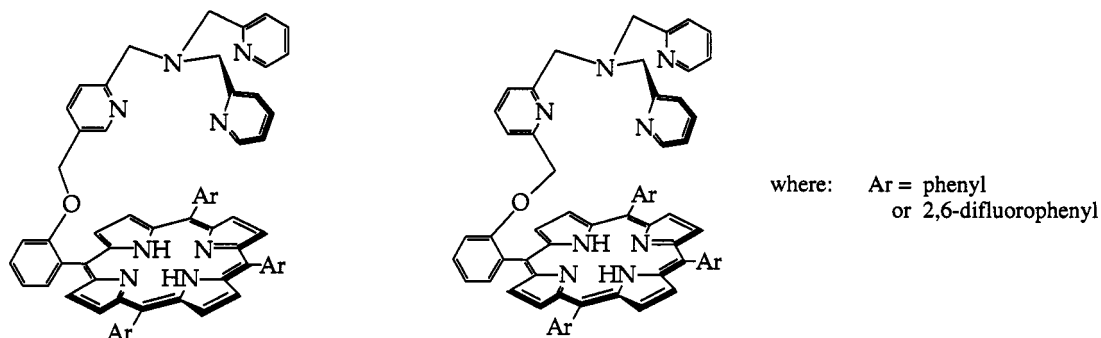


Fig. 5. Possible mechanism of formation of heterodinuclear oxo-bridged complex **9**.

Future Directions

While the "self-assembly" approach, using mononuclear iron-porphyrins and various copper-ligand complexes, will continue to be a viable and productive approach to modeling the CcoO_2 -binding center, an alternative approach will be to utilize synthetically derived ligands to which various chelates are tethered to the porphyrin periphery. This will allow for a more controlled approach to the chemistry of reacting dioxygen with reduced porphyrin-iron(II) and copper(I) complexes, since any O_2 -adducts, peroxo complexes, and other expected reduced dioxygen derivatives may form in an *intramolecular* fashion. To

these ends, and in order to incorporate the TMPA ligand for which the copper(I)-O₂ chemistry is very well understood (6), we have recently synthesized the tethered porphyrins pictured below. We expect a considerable body of exciting new chemistry to develop using these systems.



CONCLUSION

$[(\text{TMPA})\text{Cu}^{\text{I}}(\text{RCN})]^+$ (**1**) binds O₂ reversibly at -80 °C in EtCN or CH₂Cl₂ to give the Cu/O₂ = 2:1 (Cu:O₂) *trans*- μ -1, 2-peroxo adduct $\{[(\text{TMPA})\text{Cu}]_2(\text{O}_2)\}^{2+}$ (**2**). This structure is not that found in the biological O₂-carrier protein hemocyanin, but this and other studies indicate that biomimetic reversible O₂-binding in synthetic copper complexes can be studied, and that a number of Cu_n-O₂ binding modes are possible. The study of quinolyl analogues of TMPA reveal that ligand steric and electron-donating factors can affect the kinetics-thermodynamics, stoichiometry, and structure of the resulting O₂-adduct. Utilizing **1** or a Cu(II) analogue has allowed us to initiate modeling of the cytochrome *c* oxidase (C_oO) heterodinuclear Fe-Cu active site, and a crude functional mimic has been observed in the reaction of **1**, (F₈-TPP)Fe^{II}-pip₂ (**8**) and O₂, which produces the novel oxo-bridged complex $[(\text{F}_8\text{-TPP})\text{Fe}^{\text{III}}-(\text{O}_2)-\text{Cu}^{\text{II}}(\text{TMPA})]^+$ (**9**). It possesses interesting physical properties, including upfield paramagnetically shifted resonances assignable to the TMPA ligand. **9** can be reversibly protonated to give a hydroxo-bridged species $[(\text{F}_8\text{-TPP})\text{Fe}^{\text{III}}-(\text{OH})-\text{Cu}^{\text{II}}(\text{TMPA})]^{2+}$ (**12**). Future investigations may reveal the details of the O₂-reduction chemistry occurring in the formation of **9**, and provide exciting new C_oO biomimetic chemistry.

REFERENCES

- (1) K.D. Karlin and Z. Tyeklár, Eds., *Bioinorganic Chemistry of Copper*, Chapman & Hall, NY (1993).
- (2) K.D. Karlin, *Science*, **261**, 701-708 (1993).
- (3) N. Kitajima and Y. Moro-oka, *Chem. Rev.*, **94**, 737 (1994).
- (4) J. O. McNamara and I. Fridovich, *Nature*, **362**, 20-21 (1993).
- (5) (a) Z. Tyeklár and K.D. Karlin, *Acc. Chem. Res.*, **22**, 241-248 (1989). (b) K.D. Karlin, Z. Tyeklár, and A.D. Zuberbühler, *Bioinorganic Catalysis*, 261, Marcel Dekker, NY (1992). (c) Z. Tyeklár, and K.D. Karlin, *Bioinorganic Chemistry of Copper*, 277-291, Chapman & Hall, NY (1993).
- (6) (a) Z. Tyeklár, R. R. Jacobson, N. Wei, N. Narasimha Murthy, J. Zubieta and K. D. Karlin, *J. Am. Chem. Soc.*, **115**, 2677-2689 (1993). (b) M.J. Baldwin, P.K. Ross, J.E. Pate, Z. Tyeklár, K.D. Karlin, and E.I. Solomon, *J. Am. Chem. Soc.*, **113**, 8671-8679 (1991).
- (7) K.A. Magnus, H. Ton-That and J.E. Carpenter, *Chem. Rev.*, **94**, 727 (1994).
- (8) (a) K.D. Karlin, N. Wei, B. Jung, S. Kaderli, P. Niklaus and A.D. Zuberbühler, *J. Am. Chem. Soc.*, **115**, 9506-9514 (1993). (b) N. Wei, et al., *Inorg. Chem.*, **33**, 1953-1965 (1994).
- (9) M. Momenteau and C.A. Reed, *Chem. Rev.*, **94**, 659 (1994).
- (10) C.R. Andrew, K. P. McKillop and A.G. Sykes, *Biochim. Biophys. Acta*, **1162**, 105-114 (1993).
- (11) J. W. Egan, Jr. et al., *J. Am. Chem. Soc.*, **112**, 2445-2446 (1990).
- (12) (a) G.T. Babcock and M. Wikström, *Nature*, **356**, 301-309 (1992). (b) C. Varotsis, Y. Zhang, E. H. Appelman and G. T. Babcock, *Proc. Natl. Acad. Sci. USA*, **90**, 237-241 (1993).
- (13) (a) K.D. Karlin, A. Nanthakumar, S. Fox, N.N. Murthy, N. Ravi, B.H. Huynh, R.D. Orosz and E.P. Day, *J. Am. Chem. Soc.*, **116**, 4753-4763 (1994). (b) A. Nanthakumar et al., *J. Am. Chem. Soc.*, **115**, 8513 (1993).
- (14) I. Bertini, P. Turano and A. J. Vila, *Chem. Rev.*, **93**, 2833-2932 (1993); C. Luchinat and S. Ciurli, in *Biological Magnetic Resonance*, Vol. 12, L.J. Berliner & J. Reuben, eds., Plenum: NY, p 357 (1993).